



## Investigating the Adsorption of the Thyroid Stimulating Hormones Molecules on Graphene Sheets by the Density Functional Theory for Possible Nano-Biosensor Applications

Nadia Mahmoudi Khatir\* , Hooman Fatoorehchi , Aidin Ahmadi , A Khoshnoodfar , Mahdi Faghihnasiri

1. Department of Biotechnology, Faculty of Biological Science, Alzahra University, Tehran, Iran. E-mail: n.khatir@alzahra.ac.ir
2. School of Chemical Engineering, College of Engineering, University of Tehran, Tehran, Iran. E-mail: hfatoorehchi@ut.ac.ir
3. Computational Materials Science Laboratory, Nano Research and Training Center, NRTC, Iran. E-mail: aidin.ahmadiiii@gmail.com
4. Department of Biotechnology, Faculty of Biological Science, Alzahra University, Tehran, Iran. E-mail: akhoshnoodfar72@gmail.com
5. Computational Materials Science Laboratory, Nano Research and Training Center, NRTC, Iran. E-mail: mahdi.faghihnasiri@gmail.com

ARTICLE INFO	ABSTRACT
<p><b>Article History:</b> Received: 29 June 2020 Revised: 08 July 2021 Accepted: 31 October 2021</p> <p><b>Article type:</b> Research</p> <p><b>Keywords:</b> Density Functional Theory, Graphene, <math>\psi</math>-Graphene, I-V Characteristics Nano-Biosensor Thyroid Hormones Adsorption</p>	<p>In this paper, the electronic effects of the adsorption of thyroid-stimulating hormones (TSH) on two-dimensional structures of graphene and <math>\psi</math>-graphene are theoretically investigated utilizing the density functional theory (DFT). Initially, the binding energies of TSH molecules on graphene (both the zigzag and armchair structures) and <math>\psi</math>-graphene are computed at different spatial orientations using the Siesta code. The most stable orientations had the following binding energies: <math>-1.04</math> eV for triiodothyronine on graphene, <math>-1.25</math> eV for thyroxine on graphene, <math>-0.97</math> eV for triiodothyronine on <math>\psi</math>-graphene, and <math>-0.95</math> eV for thyroxine on <math>\psi</math>-graphene. After identifying the most stable orientations, the current-voltage characteristics of graphene and <math>\psi</math>-graphene monolayers, before and after the adsorption of TSH molecules are calculated by the TranSiesta computational software package, using the non-equilibrium Green's function approach. The adsorption of the TSH molecules on both graphene structures reduced the passing electric current significantly. The findings show that graphene sheets can be used to synthesize fast responding TSH nano-biosensors.</p>

### Introduction

According to the WHO, more than 200 million people in the world are affected by thyroid-related disorders. These dysfunctions include hyperthyroidism, hypothyroidism, goiter, thyroid gland tumors (benign and malignant), and subclinical hypothyroidism [1].

The diagnosis of the disorders mentioned above can be established through accurately measuring the levels of two thyroid hormones, namely triiodothyronine ( $T_3$ ) and thyroxine ( $T_4$ ), in the blood. The conventional test for such determinations is a time-consuming process, taking

\* Corresponding Author: N. Mahmoudi Khatir (E-mail address: n.khatir@alzahra.ac.ir)



several to 14 days. Providing the pediatricians with the test results for a newborn infant in a shorter time would be highly beneficial. Consequently, many research works have been focused on devising sensing systems for fast detection and measurement of triiodothyronine and thyroxine.

In 2003, Wu et al. [2] managed to synthesize a glassy carbon electrode coated with multi-walled carbon nanotubes (MWNT), whose electrochemical performance was sensitive to the thyroxine concentration. The mentioned electrode system can resemble an electrochemical sensor for thyroxine.

Wang et al. [3] in 2013 improved the performance of an interdigitated microelectrodes biosensor by incorporating nanodot arrays. The fabricated biosensor was able to detect TSH in levels as low as 0.005 mIU/l.

In 2015, Chou et al. [4] came up with an electrochemiluminescence immunosensor comprised of T3-conjugated, silver nanoparticle-decorated carboxylic graphene oxide as the carrier and anti-T3 antibody-tris(2,2'-bipyridyl) ruthenium(II) (Ru(bpy)<sub>3</sub><sup>2+</sup>) as the probe. They conclude the sensor to be ultrasensitive to TSH and operational in the concentration range of 0.1 pg/mL to 0.8 ng/mL with a detection limit of 0.05 pg/mL.

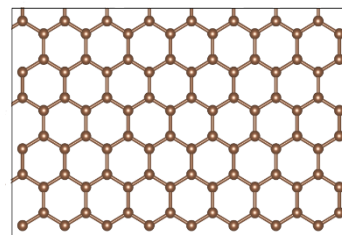
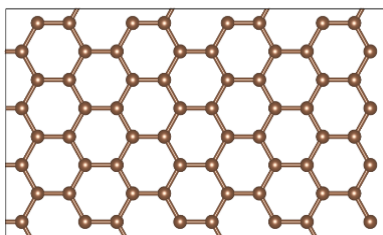
Even though DFT applies to biological science [5, 6], biosensor [7], engineering, such as chemical engineering, In chemical engineering, DFT classifies material properties and structure and mechanisms for phenomena such as chemical reaction and phase transformation that are otherwise impossible to measure experimentally. It is a standard tool for materials modeling [8-10].

In this paper, for the first time, we study the adsorption of triiodothyronine and thyroxine molecules on 2D structures of graphene and  $\psi$ -graphene are simulated using the density functional theory (DFT). The results give insights into the synthesis of possible T3 and T4 biosensors based on graphene sheets.

## Computational Procedure

The calculations were performed using the density functional theory (DFT) with the Siesta software package [11-14]. The Perdew calculated the exchange correlation functional–Burke–Ernzerhof (PBE) approximation within the framework of the generalized gradient approximation (GGA) [15-17]. Furthermore, the Troullier-Martin type norm-conserving pseudopotentials [18] was applied for all the atoms in our calculations.

As for the simulation procedure, firstly, we modeled the unit cell of graphene and  $\psi$ -graphene both in zigzag and armchair modes. The cut-off energy was set to 50 Ry. The force between atoms is set to be less than 10<sup>-5</sup> Ry/Bohr. The wave function of atoms was extended via the single-zeta polarized (SZP) basis set, and the Monkhorst-Pack *k*-point grids (12×12×1) were employed. To investigate the adsorption of triiodothyronine and thyroxine molecules on the graphene structures, the first step was to produce the optimized 3×3 supercells, see Fig. 1. Next, the adsorbate molecules triiodothyronine and thyroxine were constructed in the SIESTA package; the structures are depicted in Fig. 2.



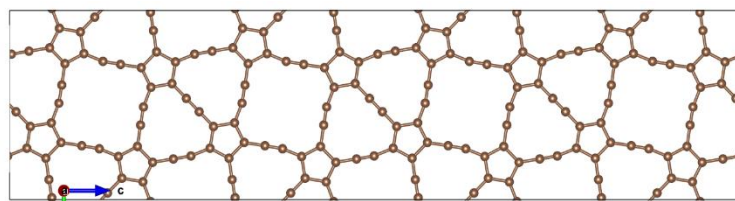


**Fig. 1.** The constructed structures of the adsorbents in the SIESTA package. Clockwise from top left: armchair graphene, zigzag graphene, and  $\psi$ -graphene

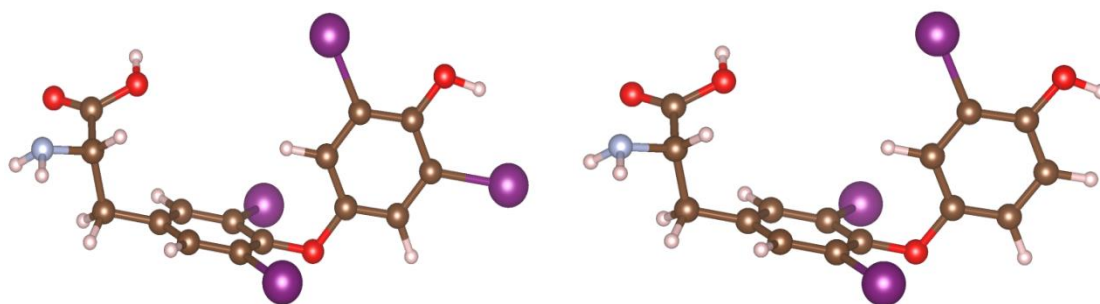


**Fig. 2.** The constructed structures of triiodothyronine (left) and thyroxine (right) molecules in the SIESTA package

The interactions between two layers of graphene and  $\psi$ -graphene is extinct by using of 20 Å vacuum. The polarization is also included in the calculations due to the existence of oxygen atoms in the structure.

As the next step, for assessing the properties of graphene as a sensor for T<sub>3</sub> and T<sub>4</sub> molecules, the current-voltage (I-V) characteristics of a relevant electrode setup using the TranSIESTA computational package were calculated [19]. The TranSIESTA package applies the non-equilibrium Green's function approach for obtaining the electron transport of compounds. The binding energy of the graphene monolayers and triiodothyronine and thyroxine molecules were calculated according to the following formula:

$$E_b = E_{X+graphene} - E_X - E_{graphene} \quad (1)$$

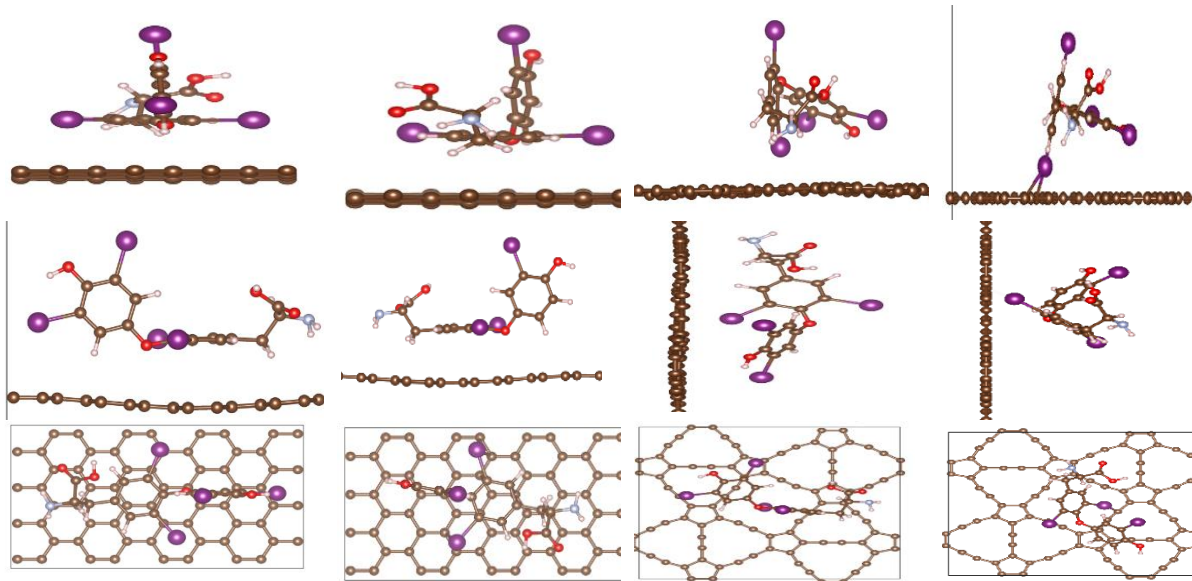
where  $E_{X+graphene}$  denotes the total energy of triiodothyronine or thyroxine (adsorbent) adsorbed onto  $\psi$ -graphene (adsorbent),  $E_X$  is the total energy of the adsorbent molecule, and  $E_{graphene}$  stands for the total energy of the virgin adsorbent.

## Results and Discussion

The previously reported results show the graphene and  $\psi$ -graphene cells in the zigzag and armchair structures [14]. The binding energies of the adsorbate molecules toward the graphene sheets at the optimal spatial orientations, as depicted in Fig. 3, were computed. The relevant numerical values of the aforementioned binding energies are listed in Table 1.

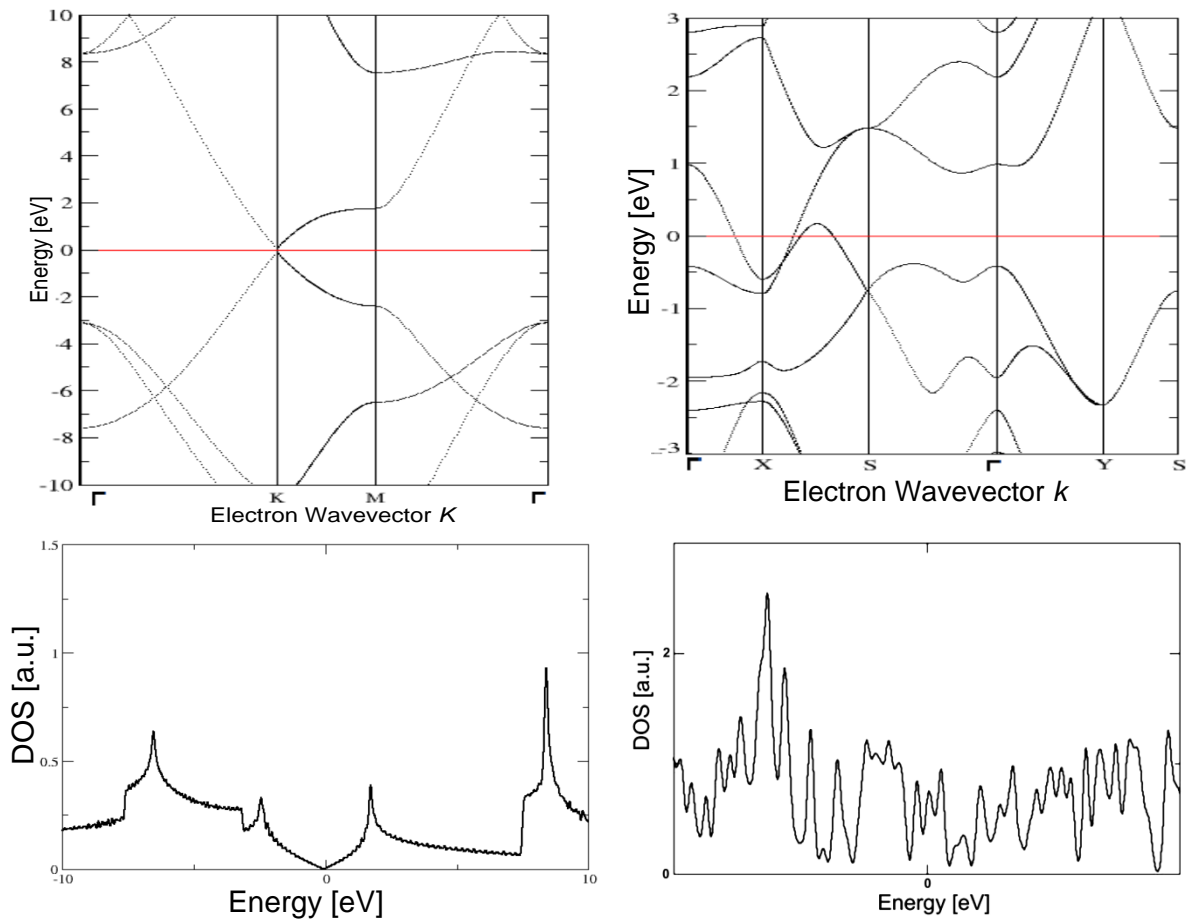
**Table 1.** Binding energies (enthalpy change of adsorption) of the TSH molecules on graphene and  $\psi$ -graphene sheets.

Case	$E_b$ [eV]
triiodothyronine on graphene	-1.04
thyroxine on graphene	-1.25
triiodothyronine on $\psi$ -graphene	-0.97
thyroxine on $\psi$ -graphene	-0.95



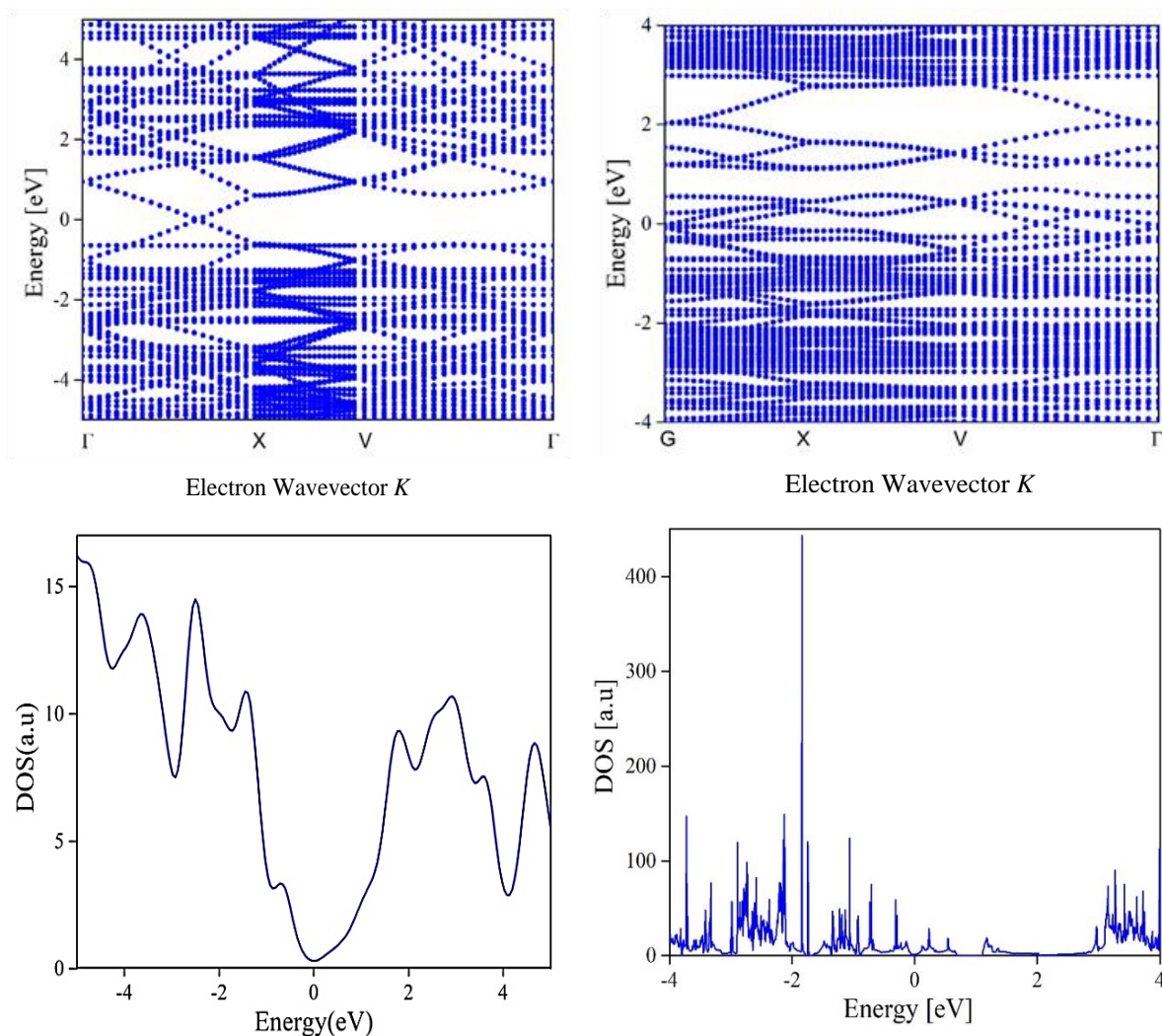
**Fig. 3.** The most stable spatial orientations of the adsorbates in the vicinity of the graphene sheets. The first column (from left): thyroxine and graphene, the second column: triiodothyronine and graphene, the third column: thyroxine and  $\psi$ -graphene, the fourth column: triiodothyronine and  $\psi$ -graphene

Subsequently, the band structure and the density of state (DOS) diagrams for graphene and  $\psi$ -graphene in pure form (Fig. 4) and with molecules adsorbed on them (Figs. 5 and 6) were obtained.



**Fig. 4.** The electronic band structure and DOS diagrams of pure graphene (left column) and pure  $\psi$ -graphene (right column)

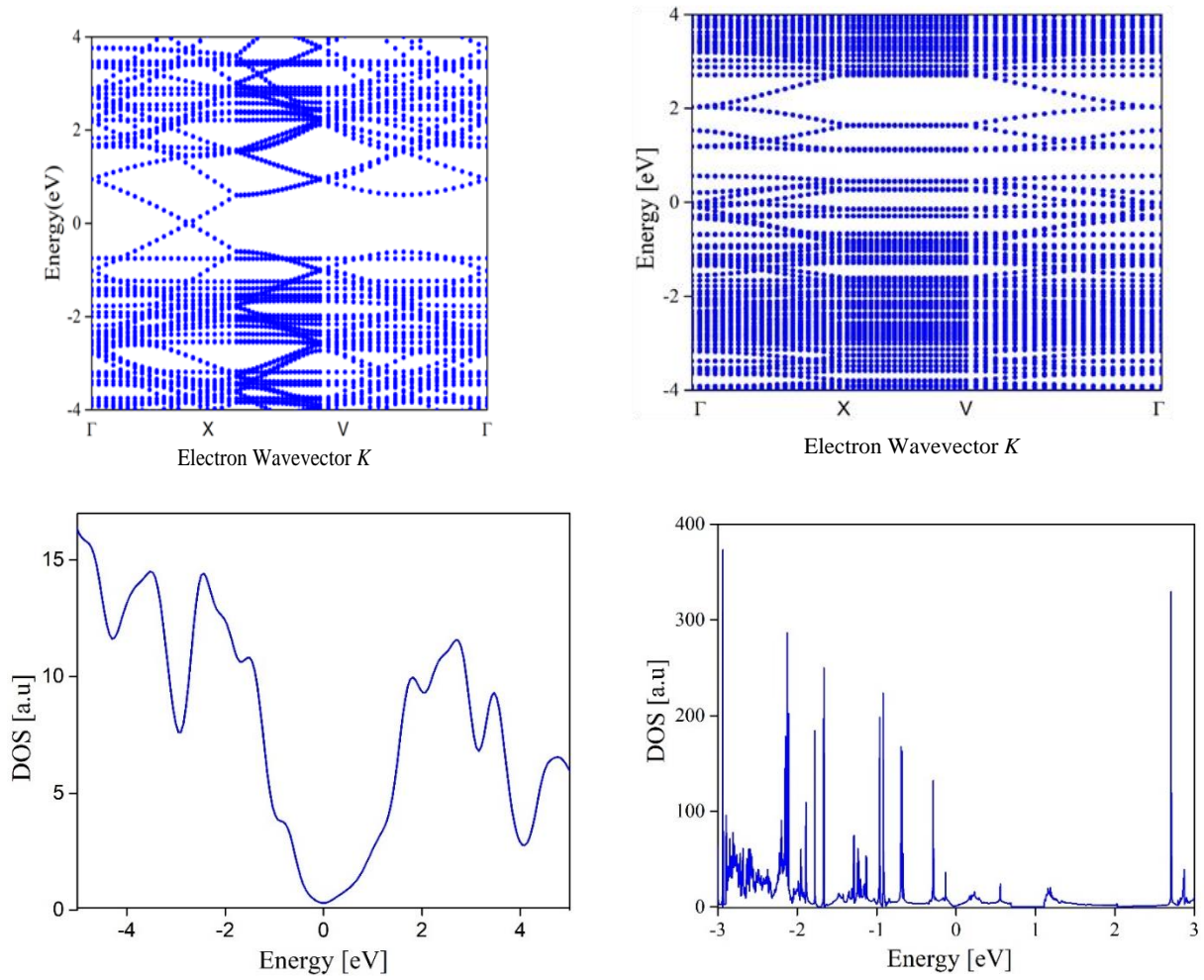
According to Fig. 4, pure graphene is intrinsic, also referred to as undoped, semiconductor. On the other hand,  $\psi$ -graphene has a substantial density of state at the Fermi level, and hence it is a conductive metal.



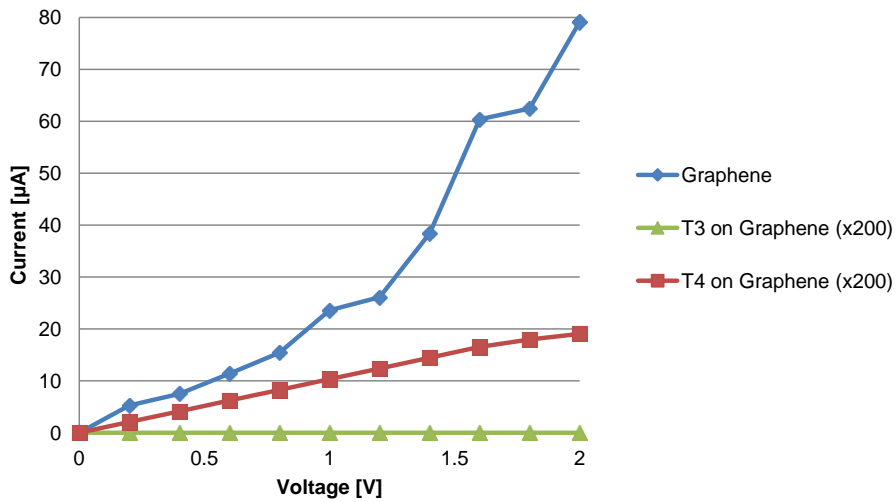
**Fig. 5.** The electronic band structure and DOS diagrams for the adsorption of triiodothyronine on graphene (left column) and  $\psi$ -graphene (right column)

The adsorbed triiodothyronine on the graphene acts as a semi-metal as there is a negligible, but non-zero, density of state at the Fermi level; see Fig. 5. Nevertheless, the two compounds constitute a semi-conductor once adsorbed on the  $\psi$ -graphene.

According to Fig. 6, the adsorbed thyroxine on the graphene and the  $\psi$ -graphene behave typically like a semi-conductor.



**Fig. 6.** The electronic band structure and DOS diagrams for the adsorption of thyroxine on graphene (left column) and  $\psi$ -graphene (right column)



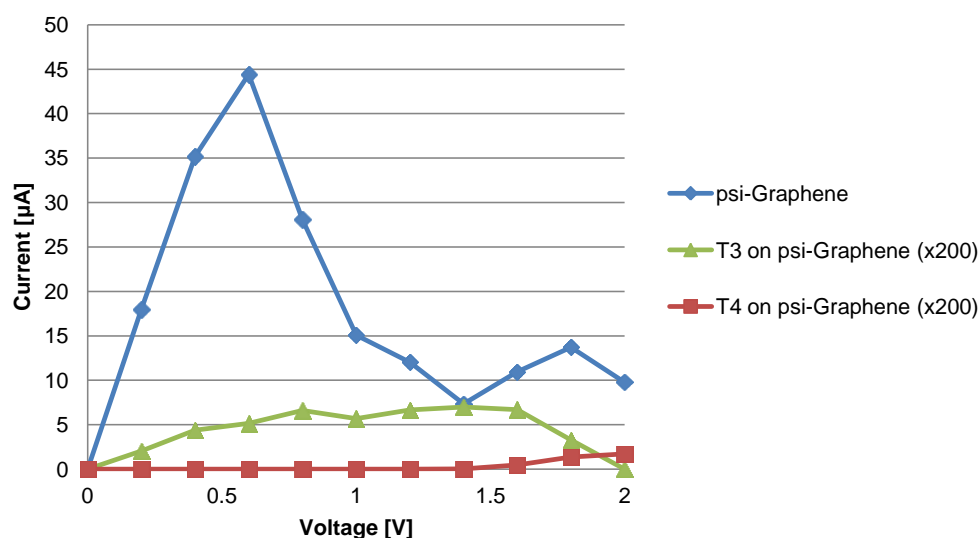


**Fig. 7.** The I-V characteristics of a setup of sheets of graphene and  $\psi$ -graphene with adsorbed triiodothyronine and thyroxine. The data of electric currents for triiodothyronine and thyroxine are multiplied by a factor of 200 for better readability

From Fig. 7, we can see that the adsorption of both triiodothyronine and thyroxine on graphene and  $\psi$ -graphene causes a reduction in electric current. However, the graphene electrodes realize an excellent differential identification of triiodothyronine and thyroxine molecules on the whole 0 to 2 volts window. Therefore, a nano-biosensor comprising of zigzag graphene nanoribbons can detect and consequently measure thyroid-stimulating hormones accurately.

## Conclusion

The adsorption of triiodothyronine and thyroxine on monolayers of graphene and  $\psi$ -graphene was studied by DFT. We can conclude that the  $\psi$ -graphene physisorbed the TSH molecules, as the corresponding binding energies were less than 1 eV, while the graphene exhibited weak chemical adsorption. The I-V characteristics of the adsorbate-adsorbent systems were calculated using the TranSIESTA computational package. The remarkable and unique current reduction was observed once the molecules were adsorbed. According to our results, graphene can be used to synthesize disposable nano-biosensors for triiodothyronine and thyroxine in wide (0 to 2) voltage window in the I-V diagram. Alternatively, reusable nano-biosensors for detection of the aforementioned molecules can be designed using  $\psi$ -graphene in a 0 to 1 volt range. Both sensors provide dependable micro amperes readings.

## References

- [1] Toft AD. Subclinical hyperthyroidism. *New England Journal of Medicine*. 2001;345(7):512-6.
- [2] Wu K, Ji X, Fei J, Hu S. The fabrication of a carbon nanotube film on a glassy carbon electrode and its application to determining thyroxine. *Nanotechnology*. 2003;15(3):287.
- [3] Wang H, Dong P, Di D, Wang C, Liu Y, Chen J, et al. Interdigitated microelectrodes biosensor with nanodot arrays for thyroid-stimulating hormone detection. *Micro & Nano Letters*. 2013;8(1):11-4.
- [4] Chou H-T, Fu C-Y, Lee C-Y, Tai N-H, Chang H-Y. An ultrasensitive sandwich type electrochemiluminescence immunosensor for triiodothyronine detection using silver nanoparticle-decorated graphene oxide as a nanocarrier. *Biosensors and Bioelectronics*. 2015;71:476-82.



- [5] Elstner M, Frauenheim T, Suhai S. An approximate DFT method for QM/MM simulations of biological structures and processes. *Journal of Molecular Structure: THEOCHEM*. 2003;632(1-3):29-41.
- [6] Salihović M, Huseinović S, Špirtović-Halilović S, Osmanović A, Dedić A, Ašimović Z, et al. DFT study and biological activity of some methylxanthines. *Bulletin of the Chemists and Technologists of Bosnia and Herzegovina*. 2014;42:31-6.
- [7] Mirzaei M, Gulseren O, Rafienia M, Zare A. Nanocarbon-assisted biosensor for diagnosis of exhaled biomarkers of lung cancer: DFT approach. *Eurasian Chemical Communications*. 2021;3(3):154-61.
- [8] Al-Mahayni H, Wang X, Harvey JP, Patience GS, Seifitokaldani A. Experimental methods in chemical engineering: Density functional theory—DFT. *The Canadian Journal of Chemical Engineering*.
- [9] Bain A, Languri E, Padmanabhan V, Davidson J, Kerns D, editors. *Thermal Conductance of Nanoparticles: A Study of Phonon Transport in Functionalized Nanodiamond Suspensions*. ASME International Mechanical Engineering Congress and Exposition; 2020: American Society of Mechanical Engineers.
- [10] Khan S, Choi H, Kim D, Lee SY, Zhu Q, Zhang J, et al. Self-assembled heterojunction of metal sulfides for improved photocatalysis. *Chemical Engineering Journal*. 2020;395:125092.
- [11] Ślusarski T, Brzostowski B, Tomecka DM, Kamieniarz G. Application of the package SIESTA to linear models of a molecular chromium-based ring. *Acta Physica Polonica A*. 2010;118(5):967-8.
- [12] Sutton JE, Panagiotopoulou P, Verykios XE, Vlachos DG. Combined DFT, microkinetic, and experimental study of ethanol steam reforming on Pt. *The Journal of Physical Chemistry C*. 2013;117(9):4691-706.
- [13] García A, Papior N, Akhtar A, Artacho E, Blum V, Bosoni E, et al. Siesta: Recent developments and applications. *The Journal of chemical physics*. 2020;152(20):204108.
- [14] Khatir NM, Ahmadi A, Taghizade N, Faghinasiri M. Electronic transport properties of nanoribbons of graphene and  $\psi$ -graphene-based lactate nanobiosensor. *Superlattices and Microstructures*. 2020;145:106603.
- [15] Perdew JP, Burke K, Ernzerhof M. Generalized gradient approximation made simple. *Physical review letters*. 1996;77(18):3865.
- [16] Gerrits N, Smeets EW, Vuckovic S, Powell AD, Doblhoff-Dier K, Kroes G-J. Density functional theory for molecule–metal surface reactions: When does the generalized gradient approximation get it right, and what to do if it does not. *The journal of physical chemistry letters*. 2020;11(24):10552-60.
- [17] Patra A, Patra B, Constantin LA, Samal P. Electronic band structure of layers within meta generalized gradient approximation of density functionals. *Physical Review B*. 2020;102(4):045135.
- [18] Troullier N, Martins JL. Efficient pseudopotentials for plane-wave calculations. *Physical review B*. 1991;43(3):1993.
- [19] Papior N, Lorente N, Frederiksen T, García A, Brandbyge M. Improvements on non-equilibrium and transport Green function techniques: The next-generation transiesta. *Computer Physics Communications*. 2017;212:8-24.

**How to cite:** Mahmoudi Khatir N, Fatoorehchi H, = Ahmadi A, Khoshnoodfar A, Faghinasiri M. Investigating the adsorption of the thyroid stimulating hormones molecules on graphene sheets by the density functional theory for possible nano-biosensor applications. *Journal of Chemical and Petroleum Engineering*. 2021; 55(2): 385-392.